Demonstration of a domestic photovoltaic-thermal (PVT)-heat pump system, performance simulation, and economic analysis for different climates

Ioannis Sifnaios, Adam R. Jensen, Mark Dannemand, Janne Dragsted

DTU Civil Engineering, Technical University of Denmark, Kgs. Lyngby [Denmark]

Abstract

In recent years, there has been a growing interest in heat pumps coupled with photovoltaic thermal (PVT) collectors to cover the space heating and domestic hot water demand in buildings. However, most existing systems have not been designed for the specific heat demand of the climate they are located, and limited system comparisons have been conducted regarding performance and economy in different locations. In this study, the performance of a domestic PVT heat pump system installed in Denmark was demonstrated. A TRNSYS model of the system was created and validated with experimental data from the demonstration system. Afterward, it was used to perform a sensitivity analysis on the collector area to achieve the best performance and economy, using multiple indicators. Three different systems were investigated in three locations: a PVT water-source heat pump system, a photovoltaic (PV) air-source heat pump system, and an air-source heat pump system in Denmark, Austria, and Greece.

Keywords: Solar-assisted heat pump, TRNSYS, space heating, domestic hot water, PVT

1. Introduction

In Europe, almost 30% of the total energy consumed is used for space heating (SH) and domestic hot water (DHW) production. As of 2017, 9% of the energy used for SH and DHW is supplied by district heating (DH) (Fraunhofer Institute ISI, 2017). In Denmark, DH delivers heat to more than 60% of residential consumers (Danish Energy Agency, 2017). However, DH is not always available or feasible; hence, many consumers rely on individual oil, gas, and biomass boilers or heat pumps. For consumers who do not have access to DH, heat pumps are encouraged. They have generally been considered an efficient and sustainable solution since a large share of Denmark's electricity production comes from renewable energy sources (Danish Energy Agency, 2017).

Historically, ground and air source heat pumps have dominated the market. However, several manufacturers have developed hybrid Photovoltaic-thermal (PVT) collectors specifically for coupling with heat pumps in recent years. An advantage of PVT collectors is that they can produce electrical and thermal energy simultaneously (Aste et al., 2014). Like solar thermal (ST), PVT collectors can be coupled to heat pumps for covering the SH and DHW demand in buildings and are usually referred to as solar-assisted heat pump (SAHP) systems. PVT or ST collectors are typically connected to the source side of the heat pump, resulting in a higher source temperature, which increases the Coefficient of Performance (COP) of the heat pump, leading to lower operating costs (Pärisch et al., 2014).

Several studies have investigated SAHP systems, comparing systems located in different geographical locations, agreeing that PVT systems are attractive regarding performance and economy in countries with high solar irradiance and high ambient air temperatures (Fine et al., 2017; Ramos et al., 2017). However, in most of these studies, a sensitivity analysis of the system has not been performed, so it is unclear if these systems are optimized for the specific heat demand of the climate they are located. Proper dimensioning of the system's components has been proven very important for the performance of a system. A study performing sensitivity analyses on SAHP systems found that appropriate sizing of the system components can dramatically affect the system's performance, improving thermal performance by 18% and electrical performance by 50% (Dannemand et al., 2020).

This study aims to evaluate the performance of a pilot DHW and SH system consisting of building integrated PVT collectors connected to a water-source heat pump. A techno-economic analysis was carried out through simulations, where the system components were varied in size, and key performance indicators (KPIs) were calculated. Following this, the KPIs of the pilot system were compared to a system with an air-source heat pump and PV panels and a reference system with an air-source heat pump. Further, the analysis included simulations of these systems for the Northern, Central, and Southern European climate, elucidating the strengths and weaknesses of each system in each climate. Such studies are limited to the authors' knowledge, despite their great interest in industry and academia.

2. Methods

Initially, the performance of a pilot PVT – heat pump system was investigated. Afterward, a model of the pilot PVT – heat pump system was created in TRNSYS 18. The model's performance was compared to the measurements from the pilot system to have the model perform as close to the existing system as possible. Subsequently, a sensitivity analysis of the size of the PVT area was performed using reference year weather data. The results were compared to a reference system with an air-to-water heat pump and an alternative system where the air-to-water heat pump was coupled to PV panels. The comparison was made in terms of performance and economy for three different locations in Europe, namely Denmark, Greece, and Austria.

2.1 Pilot system description

The system under investigation was a roof-integrated PVT – heat pump system installed in a row house in Ølstykke, Denmark (55.777° N, 12.169° E). The 101-m^2 house was built in 1983 and was the residence of a four-person family. The PVT – heat pump system was installed as part of a completed demonstration project. The performance of the investigated system was monitored for a period of seven months, from January to July of 2019. However, the system is still in operation until the time of writing.

The system consisted of a building integrated PVT roof with a 25° tilt, shown in Fig. 1(a), connected to a heat pump. On the south side of the roof, 16 unglazed PTV panels were installed with an area of 48 m², along with four dummy panels to achieve a consistent aesthetic result. The PVT panels installed on the roof are numbered in Fig. 1(a) to be more visible. Two of these 16 panels were not in operation (panel numbers 5 and 13); thus, the active PVT area was 42 m^2, corresponding to 14 panels. The PVT panels were south-west oriented (192° from the north) and were installed in seven rows of two in parallel. On the north side of the roof, 16 PV panels were installed, but they were not included in this study since they were not in operation during the monitoring period of the system. Fig. 1(b) illustrates a schematic of the system under investigation.
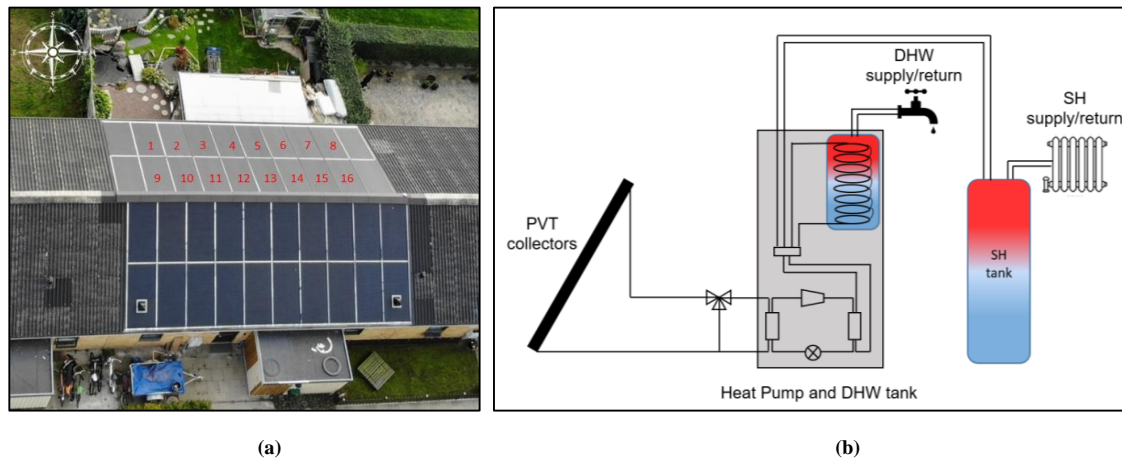

| (a) | (b) |

Fig. 1: Aerial photo of the roof integrated PVT panels (a) and schematic of the pilot system (b).

2.2 System control

The system was controlled through the following parameters and settings:

- The heat pump was set in operation when it had to charge the DWH or the SH tank. Charging of the DHW tank always had priority over the SH tank.

- The DHW tank was charged when the bottom temperature was lower than 44 °C and stopped when the top was higher than 59 °C.

- The SH tank was charged when the top temperature was lower than $SH_{setpoint} - 4$ K, and charging stopped when the bottom temperature was higher than $SH_{setpoint} + 4$ K.

- The $SH_{setpoint}$ was based on the ambient temperature (T_{amb}) and was calculated from the following equation:

$$SH_{setpoint} = 51.42 - 0.4025 \cdot T_{amb} - 0.0197 \cdot T_{amb}^2 - 7 \cdot 10^{-4} \cdot T_{amb}^3 \qquad \text{(eq.1)}$$

Equation (1) was obtained by least-square fitting a third-order polynomial to the manufacturer-specified space heating setpoints as a function of temperature. The space heating temperature set points were obtained through the online heat pump website portal. The described control strategy was implemented in the developed TRNSYS model

of the system.

2.3 TRNSYS model

A simulation model of the pilot system was developed in the simulation software TRNSYS 18. The model was validated with measurements for two weeks, namely from 14/2/2019 to 28/2/2019. The reason for choosing this period was that since the system was located in an inhabited house and was observed remotely, there were many situations where technical errors occurred during data acquisition, leading to very few periods with data available for all the components. The two weeks in February were the longest continuous period with all data available, and thus it was selected for model validation. An overview of the TRNSYS model is presented in Fig. 2.
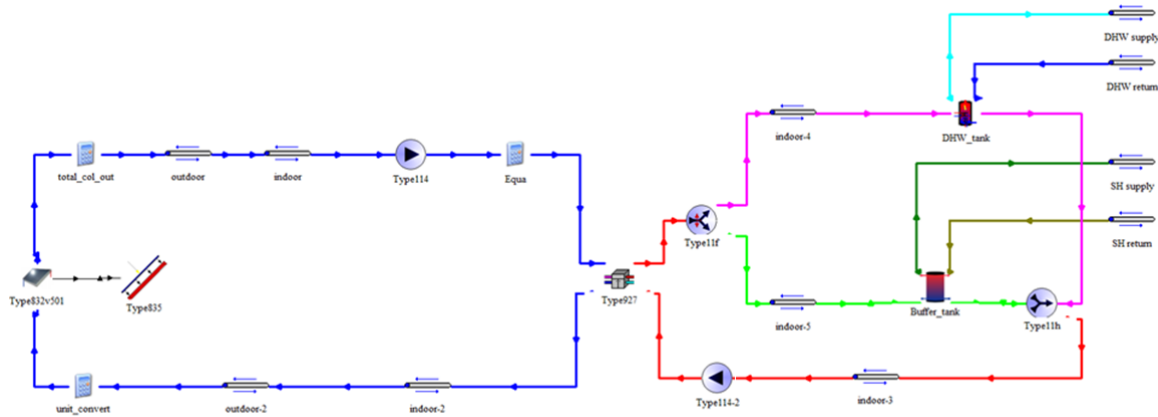

Fig. 2: TRNSYS model of the system.

For modeling the PVT collector, TRNSYS component Type 835 (Danny, 2018) was used to simulate the electrical output, and Type 832 (Haller et al., 2012) was used to simulate the thermal output. Type 832 calculates the thermal output using the coefficients from the Quasi dynamic modeling method, as described in ISO 9806:2017 (International Organization for Standardization, 2017). In addition, it calculates the mean temperature of the collector fluid in the absorber, which is then given as input to Type 835 to calculate the PV cell temperature and thus the electrical output of the collector.

Since the panels were installed in parallel, in seven rows of two, in the TRNSYS model, for the ST part, the output of one row of collectors was simulated and multiplied by seven to get the output of all seven rows. The available measurements of weather conditions were limited, and only the total irradiance in the collector plane and the ambient temperature was available. The parameters for simulating the PVT collectors are presented in Tab. 1. It can be noticed that the used heat loss coefficient is significantly higher than typical values in the literature, where the heat loss factor is around 13 W/m^{2}K for unglazed PVT collectors (Lämmle et al., 2017). This increased value was used because it included the heat losses caused by the wind. Since the PVT collectors were unglazed, heat losses due to wind were significant. However, wind measurements were not available on-site, so their effect was incorporated in the heat losses.

Tab. 1: Parameters used for modeling of PVT collector used in Type 835 and Type 832.

Parameter	Value	Unit
Optical efficiency	0.54	-
Linear heat loss coefficient	18	W/m^{2}K
Effective thermal capacity	60	kJ/m^{2}K
Electrical efficiency at reference conditions	0.18	-
Temperature coefficient of solar cell efficiency	-0.4	%/K
Irradiance dependence of PV efficiency	-0.00035	W/m^{2}K

The TRNSYS component Type 927 was used to simulate the heat pump operation. A TRNSYS component for simulating the operation of a water-to-water modulating heat pump does not exist at the time of writing. For this reason, the modulating operation was modeled using a scale factor for regulating the heat pump capacity according to the desired output temperature and the inlet temperature of the source and load side, as is suggested in the literature (Dannemand et al., 2020). In addition, a constant electricity consumption of 22 W per hour was added to the

consumption of the heat pump to account for standby operation and electricity consumption of the circulation pump. Last, using an equation in TRNSYS, the source temperature entering the heat pump was limited to 20 °C, to account for the actual heat pump operation.

The DHW tank was simulated using TRNSYS Type 340, having a volume of 180 L and a height of 1.3 m. These values correspond to the actual dimensions of the DHW tank in the pilot system. The cold-water inlet was located at the bottom of the tank, and the DHW outlet at the top. The heat loss coefficient was set to 2 W/K for the top of the tank, 1.7 W/K for the sides, and 1.2 W/K for the bottom. These values were set so that the measured energy consumption for DHW matched the value obtained from the simulation. The HP charged the tank through a spiral heat exchanger.

A similar procedure was used for simulating the SH tank where Type 534 was selected, having a volume of 100 L and a height of 1.2 m. The heat losses were set to 2 W/K for the top of the tank, 1.6 W/K for the sides, and 1.1 W/K for the bottom. The SH tank was charged directly from the heat pump without the use of a heat exchanger. Hot water was taken from the top of the tank and supplied to the SH loop, while the loop's return was inserted in the bottom.

Both tank components divide the tank volume into a finite number of isothermal nodes, where each node is affected by fluid conduction, temperature inversion, and inlet/outlet flows. Stratification within the tanks is determined by the temperatures supplied to the tank and the number of nodes specified. The number of nodes for each tank was chosen based on the best results when comparing the outlet temperature. This resulted in 100 nodes for the DHW tank and 50 nodes for the SH tank, corresponding to 1.2 L and 2 L per node, respectively.

The system's thermal capacity and heat losses were modeled with 22 m of pipe on the source side of the heat pump (12 m exposed to outdoor ambient temperature and 10 m to indoor) and 1 m pipe connecting the heat pump with each tank.

2.4 TRNSYS model for yearly performance

The yearly simulation was performed using the Meteonorm weather files in TRNSYS. The SH setpoint was calculated from the ambient temperature, as described in equation (1). The SH heat load was 6 kW at an outdoor temperature of -10 °C and 0 kW for 18 °C or higher.

The DHW profile for the annual simulation in TRNSYS was created using the software DHWcalc from IEA Task 26 (Jordan and Vajen, 2001). The software generates daily DHW profiles by distributing DHW draw-offs throughout the year according to a probability function (Jordan and Vajen, 2000). The draw-offs are not identical for each day, whereas the total water volume is the same. In the yearly TRNSYS simulation, the daily DHW draw-off was set to 120 L, a typical value for a single-family house in Denmark.

2.5 Investigated scenarios

A sensitivity analysis was performed on collector areas ranging from $10 - 40\ m^2$ to identify the PVT area that gives the best performance and economy for the pilot system. The heat pump of the pilot system was oversized; thus, smaller heat pumps were investigated in the simulations. Assuming that the ratio of the minimum load to the nominal capacity is 20 – 30% for most modulating heat pumps, a heat pump of 1.2 – 6 kW was considered most appropriate for Denmark and Austria and 0.9 – 4.5 kW for Greece.

In general, it is a common practice to use an oversized heat pump in domestic heating systems. Typically, a heat pump would be selected so the nominal capacity can match the building heat demand on the coldest day in the region. This forces the heat pump to operate in part-load capacity most of the time and minimizes the chance of direct electricity consumption through the auxiliary electrical heater, potentially resulting in a higher Seasonal Performance Factor (SPF) of the system (Zottl et al., 2012). However, in the pilot system, the minimum capacity of the heat pump was larger than the maximum heating load, so this principle was not fulfilled, as shown in Section 3.1.

The PVT-heat pump system was compared to a reference system and a PV-air-heat pump system. The reference system consisted of a modulating air-to-water heat pump (Type 509b: Variable Speed Compressor Air-to-Water Heat Pump), and the load side of the heat pump, storage tanks, and the control of the system remained the same. For simulating the heat pump, the performance map of Daikin Altherma ERLQ006-CV3 was used (Daikin, n.d.). The capacity of the air-to-water heat pump was the same as the water-to-water for the investigated locations.

The PV-air-heat pump system had the same heat pump as the reference system and 40 m^2 of PV collectors, able to supply electricity to the heat pump and the household. A sensitivity analysis on the PV collector area was performed, varying the collector area from $10 - 40\ m^2$, but only the best performing scenario is presented in this study for space-saving purposes.

2.6 Key Performance Indicators and economic analysis

To assess the system's performance under investigation, selected key performance indicators (KPIs) were calculated, giving simplified information about the system's performance. The International Energy Agency – Solar Heating & Cooling Programme – Task 60 recommended the indicators used (IEA SHC Task 60, n.d.) and are presented in Equations (2) – (8). The term heating system (*HS*) refers to the entire system under investigation except for the PVT panels.

The **net solar electrical fraction** is the ratio of electrical energy produced by the PVT, E_{PVT}, relative to the sum of the electricity consumed by the heating system and household, $E_{HS}+E_{HE}$.

$$f_{sol,el}^{net} = \frac{E_{PVT}}{E_{HS} + E_{HE}}$$
(eq.2)

The **seasonal performance factor (*SPF*)** is the thermal energy produced by the heating system, Q_{HS}, divided by the electrical energy from the grid used by the heating system $E_{grid,HS}$.

$$SPF = \frac{Q_{HS}}{E_{grid,HS}}$$
(eq.3)

The **electricity self-consumption fraction** is the ratio of the directly consumed PVT-generated electricity by the heating system and the house, $E_{PVT,HS} + E_{PVT,HE}$, to the total electricity production of the PVT, E_{PVT}.

$$f_{self,el} = \frac{E_{PVT,HS} + E_{PVT,HE}}{E_{PVT}}$$
(eq.4)

The **levelized cost of energy (*LCOE*)** measures the average net present cost of energy generation for a system over its lifetime. It is calculated as the ratio between the costs over the system's lifetime to the sum of the energy delivered.

$$LCOE = \frac{I_0 + \sum_{t=1}^{LT}\left(OM_t - RV_t - E_{PVT,grid,t} \cdot P_{el,sale,t} - E_{PVT,HE,t} \cdot P_{el,ret,t}\right) \cdot (1+r)^{-t}}{\sum_{t=1}^{LT}\left(Q_{HS,t} + E_{HE,t}\right) \cdot (1+r)^{-t}}$$
(eq.5)

Where I_0 is the initial investment cost, *OM* is the operation and maintenance cost, *RV* is the residual value, $P_{el,sale}$ is the price of electricity sold to the grid, $P_{el,ret}$ is the retail price of electricity, *r* is the discount rate, and *LT* is the lifetime of the system. In the *LCOE* expression, two things were accounted as income; the income from selling electricity to the grid and the savings deriving from the part of household electricity demand that the PVT collector covered.

The **payback period (*PP*)** corresponds to the time after which the financial savings achieved with the solar heating system compared to the reference system compensated for the additional investment for the solar heating system.

$$I_{0,sol} - I_{0,ref} = \sum_{t=1}^{PP}\left(\Delta OM_t + E_{PVT,grid,t} \cdot P_{el.sale,t} + E_{PVT,HE,t} \cdot P_{el,ret,t}\right) + \Delta RV_{LT}$$
(eq.6)

Where ΔOM_t is the difference between the operation and maintenance cost of the two systems.

$$\Delta OM_t = (OM_t)_{ref} - (OM_t)_{sol}$$
(eq.7)

And ΔRV_{LT} is the difference between the residual values of the two systems after their lifetime.

$$\Delta RV_{LT} = (RV_{LT})_{sol} - (RV_{LT})_{ref}$$
(eq.8)

2.7 Economic assumptions

For calculating the economic performance indicators, the following assumptions were made:

- The OM costs were calculated based on the electricity price and the electricity consumption of the heat pump (operation costs), plus 1% of the total investment cost of the system (maintenance costs). It has to be noted that the exact OM cost of the system are not known.

- The lifetime of the investigated system was assumed to be 25 years, which was a reasonable assumption for a solar heating system according to IEA Task 54 (IEA Task 54, 2018). The residual value was assumed zero.

- According to IEA Task 54 (IEA Task 54, 2018), since the discount rate is normally taken equal to the weighted average cost of capital (WACC) and the total cost is paid upfront for single-family systems, the discount rate was taken at 0%.

- The household electricity consumption used was from an actual building in Denmark, corresponding to 3320 kWh/year. For simplicity, the same consumption was used for all investigated locations.

The costs of the individual components used in the investigated systems are presented in Tab. 2. These prices were based on indicative retail prices of these types of components in Denmark. The heat pump cost was assumed constant and independent of the heat pump capacity to simplify the calculations. The installed panels were integrated into the roof of the building, substituting the roof material. For this reason, an amount was subtracted from the investment cost of the installation due to less roof material used. The amount was based on the m^2 of panels installed.

Tab. 2: Components' costs

Component	Cost	Unit	Source
PVT collector	268	$€/m^2$	Invoices sent to authors
PV collector	185	$€/m^2$	(Fina et al., 2020)
Heat pump (water-to-water)	8000	€	("PriceRunner," 2020)
Heat pump (air-to-water)	5400	€	(Daikin, 2017)
Pipes (including insulation)	10	€/m	(Wang et al., 2019)
Space heating tank 100 L	400	€	("VVS-Eksperten A/S," 2020)
Inverter	$22.64 \cdot A_G + 658.43$*	€	(Europe-Solarshop, n.d.)
Expansion vessel	100	€	Invoices sent to authors
Heat transfer fluid	3	€/L	(Wang et al., 2019)
Roof material saved	67	$€/m^2$	Supplied by PVT manufacturer

* The price of the inverter is calculated based on the area of the panels (A_G). This expression was derived from prices of Fronius inverters (Europe-Solarshop, n.d.), assuming that a 2 m^2 PV panel produces 350 Wp.

2.8 Location description

Systems at three different locations were studied, namely Denmark, Greece, and Austria. For simplicity, the capital of each country was used for selecting the weather file in the TRNSYS simulation, namely Copenhagen, Athens, and Vienna. However, different electricity prices and labor costs for each country affect the economic indicators. In addition, the heating periods in the countries are different due to climate differences. The space heating load for each country was calculated based on the ambient temperature. The data used for each country are presented in Tab. 3.

Tab. 3: Data for each investigated country

	Denmark	Greece	Austria
Retail electricity price	0.31 €/kWh (Danish Utility Regulator, 2019)	0.18 €/kWh (HAEE, 2019)	0.21 €/kWh (European Commission, 2019)
Wholesale electricity price	0.055 €/kWh (EnergiNet, n.d.)	0.066 €/kWh (European Commission, 2019)	0.059 €/kWh *
Installation cost	20% of the component cost (high technician salaries)	7.2% of the component cost (64% lower labor costs than Denmark (Eurostat, 2019))	15.5% of the component cost (22% lower labor costs than Denmark (Eurostat, 2019))
Heating Period	15/9 – 15/5	15/10 – 15/4	1/10 – 30/4
Capital coordinates	55.676° N, 12.568° E	37.984° N, 23.728° E	48.208° N, 16.374° E
Mean yearly temperature	7.9 °C	17.6 °C	9.8 °C
Total horizontal yearly solar irradiation	989 kWh/m^2	1565 kWh/m^2	1112 kWh/m^2

* In Austria, residential PV systems larger than 5 kWp are supported for up to 13 years with an electricity selling price of 0.08 €/kWh (Fechner, 2018). After that period, the price for selling electricity to the grid is 0.037 €/kWh (European Commission, 2019). The weighted average is taken in this study for 25 years of operation.

3. Results

3.1 Pilot system performance

The PVT-heat pump system was able to cover the total heating demand of the house. The monthly energy

consumption for space heating and domestic hot water is presented in Fig. 3(a). As expected, the space heating consumption exhibited a clear seasonal trend, with lower heat consumption in the spring and summer months.
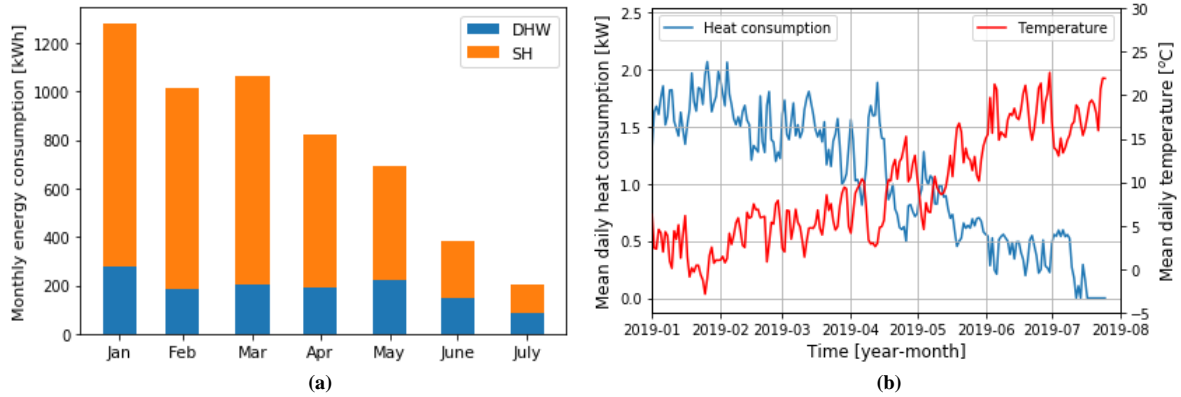

(a)

(b)

Fig. 3: Monthly energy consumption for DHW and SH (a) and mean daily SH consumption and outdoor temperature (b).

The mean daily SH consumption can be seen in Fig. 3(b). It can be observed that the mean SH load was very low compared to the size of the heat pump (3-12 kW). This indicates that the heat pump was oversized for this system, resulting in very short operation periods and relatively low heat pump efficiency. This is illustrated in Fig. 4(a), where the daily average COP of the system is presented. According to the manufacturer, the seasonal COP of the heat pump for a heating system with radiators in a cold climate (Helsinki) should be 4.3. However, for the investigated system, which was also a radiator heating system in a cold climate, a COP closer to 3 was obtained. This may be due to the oversized heat pump, which resulted in many start/stops within each day instead of continuous operation. This can be seen in Fig. 4(b), where the flow rate in the HP source loop, indicating HP operation, is presented for two days of operation. It can be observed that the heat pump had 15 to 17 operation cycles within one day.
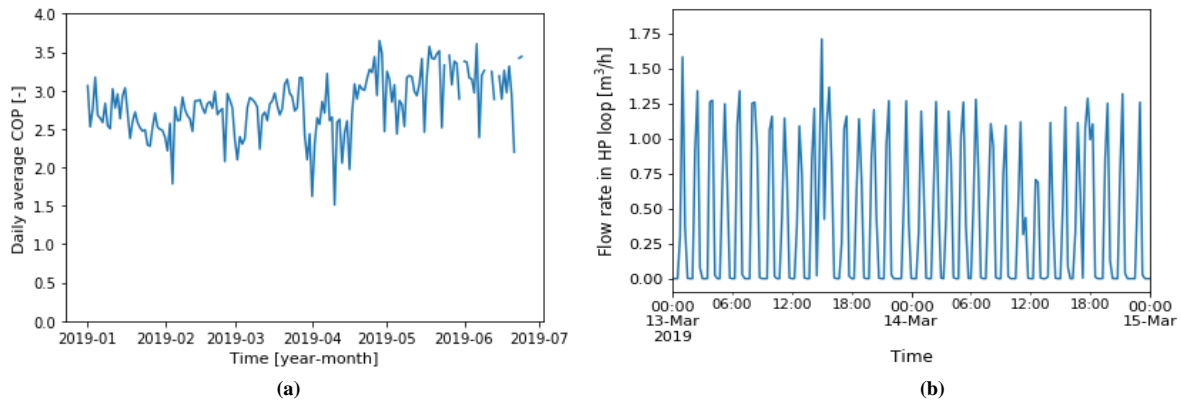

(a)

(b)

Fig. 4: Daily average COP of the system (a) and heat operation for two days (b).

3.2 TRNSYS model validation

The TRNSYS model outputs are compared to measurements from the pilot system in Fig. 5. As it can be observed, there is generally a good match between the compared parameters. The bias between the measured and modeled values for the simulated period was around 2% for all investigated parameters. The corresponding bias for each parameter is presented in Tab. 4. In general, the results of the TRNSYS simulation were in good agreement with the measured data; thus, the model was considered accurate for describing the operation of the pilot system.

Tab. 4: Variation between the measured and the simulated parameters for the investigated period.

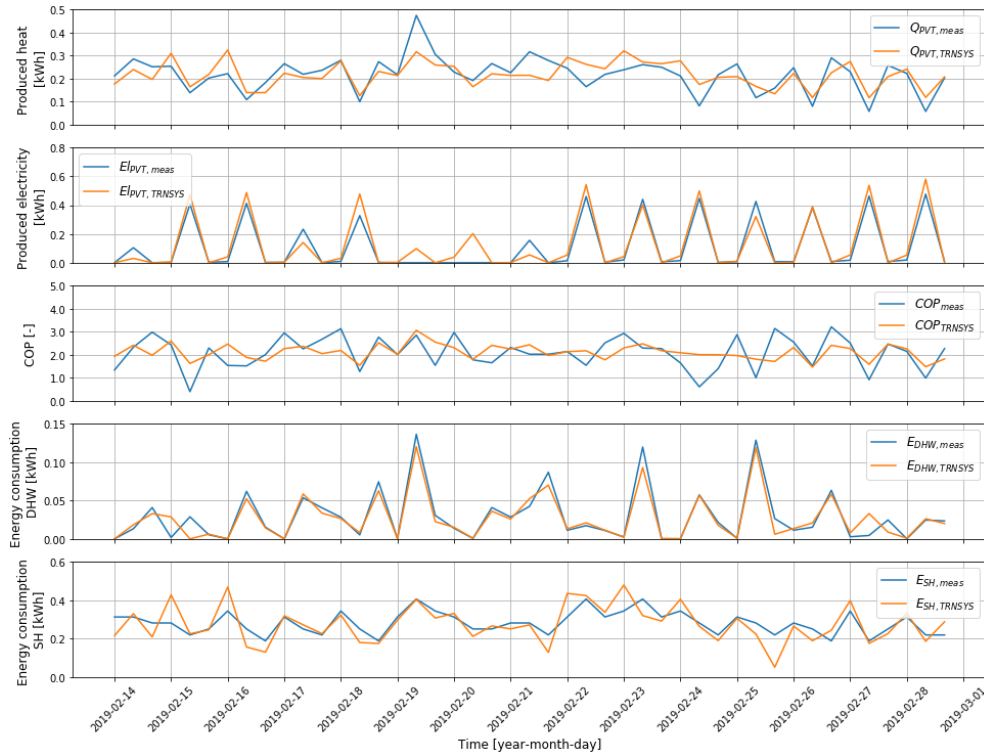| Parameter	Bias [%]
PVT collector thermal output	2.1
PVT collector electrical output	-2.1
Heat pump COP	2.2
DHW energy consumption	-2.3
SH energy consumption	-2.3

Fig. 5: Comparison of measurements from the pilot system and modeled values from the TRNSYS simulation.

3.3 System comparison

The performance indicators of the systems are presented in Fig. 6 and Fig. 7. A short description of each case, along with the economic indicators, are given in Tab. 5. The scenarios with the smaller heat pump sizes are referred to as "small" in the diagrams.

In Fig. 6, the net electricity fraction and the electricity self-consumption fraction are presented. As expected, when using smaller collector areas, the net electricity fraction was decreased while the self-consumption fraction increased. This happened because, although less electricity was produced, a larger fraction of it was used directly by the heating system or the household. The low wholesale electricity price encourages self-consumption of electricity; thus, all investigated cases maximized their profit for a self-consumption fraction of 50 – 60%. Higher self-consumption fractions were not favorable to the systems' economy since they occurred due to very low total electricity production.
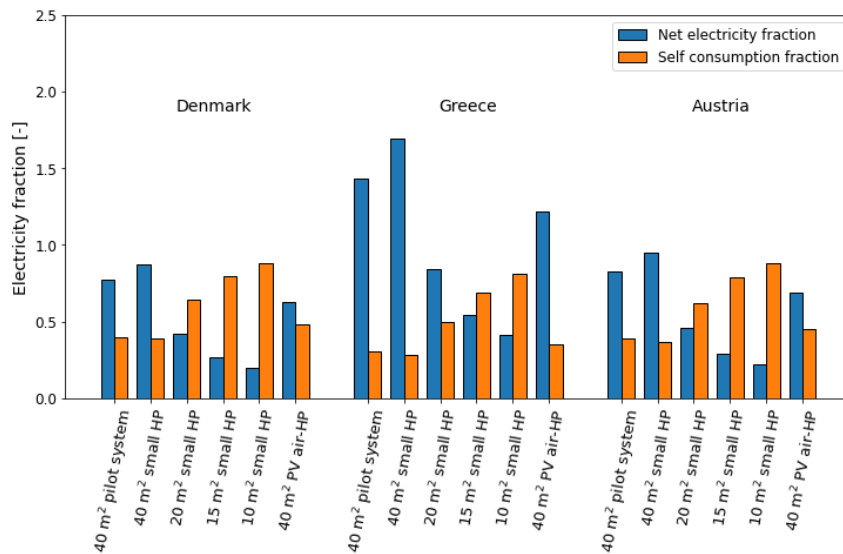

Fig. 6: Net electricity and Self-consumption fraction of the compared systems.

The SPF of the investigated systems is presented in Fig. 7. The reference system had the lowest SPF among the

investigated systems, approximately 2 in Denmark and Austria and 3 in Greece. The main reason for this is that the entire electricity consumption of the reference system comes from the grid. In contrast, the PVT and PV systems have higher SPFs since the systems consume less electricity from the grid due to self-consumption. In addition, the air-to-water HP has a relatively low COP in cold climates, especially when the HP has to produce high-temperature output. It can also be observed that the PVT-HP systems in all investigated scenarios had higher SPFs than the PV-HP system. The reason is that in PVT-HP systems, the heat pump COP is increased due to the brine temperature increase through the panel. Lastly, the effect of the HP size is also illustrated in Fig. 7, where a smaller HP always increases the SPF of the system. The largest improvement of the SPF was in Greece, where a HP with approx. 60% lower capacity, increased the SPF of the system by 95%, due to optimal operation leading to lower electricity consumption but also high self-consumption of the system.

Although the PVT water-HP systems have larger SPFs than the PV air-HP system, they are less economically attractive, having higher LCOEs and PPs, as shown in Tab. 5. The reason is that the investment costs of the PV systems are lower since the price of PV modules is 30% lower than PVT modules, the air-to-water HP is 32% cheaper than the water-to-water and has a simpler, thus cheaper, installation.

In Tab. 5, it can be observed that LCOE was lowest in Greece, followed by Austria, and highest in Denmark. This indicates the effect of high installation costs and low solar irradiance on LCOE. Countries like Greece, with high annual solar irradiance and low installation costs, had lower LCOE than countries like Denmark with low solar irradiance and high installation costs, suggesting Greece is a more favorable location for installing SAHP systems.
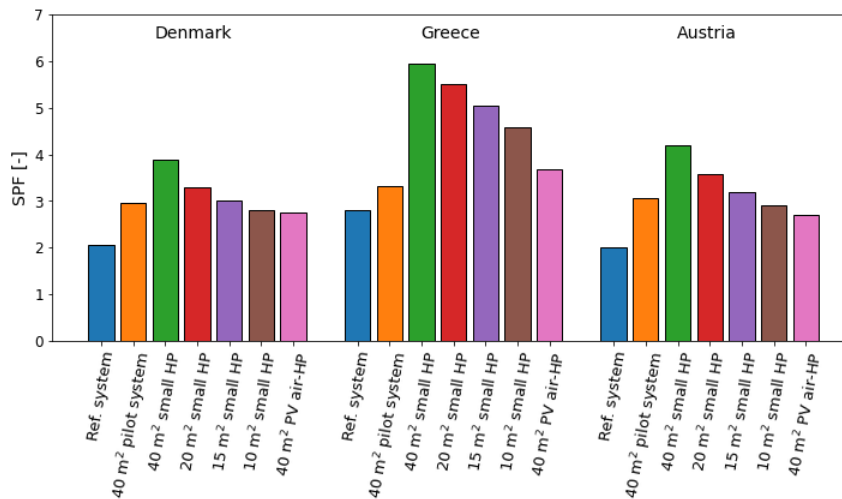

Fig. 7: SPF of the compared systems.

However, Denmark has the highest retail price of electricity, making the savings deriving from electricity self-consumption considerable. This leads to Denmark having the biggest difference between LCOE and LCOE$_{ref}$ and thus has the shortest payback period among the compared countries. Greece and Austria have longer payback periods, with values exceeding the lifetime of the system in some cases.

A big difference is spotted when comparing the LCOE of the PVT system with the LCOE of the PV system for the investigated countries. It can be observed that the LCOE of the PVT system is just 10% higher compared to the PV in Denmark and Austria but 50% higher in Greece. This finding suggests that a PV air-HP is a more suitable solution for warmer climates where the air-HP has a higher COP. PVT water-HP systems show their potential in the colder climates, indicating that they could be the optimal option had the system's price been slightly lower. In this study, the PVT collectors were assumed approximately 30% more expensive than PV panels. However, if the cost of the PVT collectors was only 15% higher than the PV panels, then the PVT water-HP systems would have a marginally lower LCOE than the PV air-HP system in Denmark and Austria. This price decrease is considered a possible scenario for the near future, as the PVT technology is currently at a relatively early stage in development compared to the more mature PV technology.

Lastly, it has to be mentioned that the best performing SAHP systems have lower LCOE than the reference system in all countries, indicating that they are a more suitable choice than an air-to-water HP, regardless of the climate they are installed in.

Tab. 5: Levelized cost of energy (LCOE) and payback period (PP) of the investigated cases.

	System	Panel Type	HP capacity [kW]	HP type	LCOE [€/kWh]	PP [years]
Denmark	Reference system	-	1.2 - 6	Air-to-water	0.14	-
	40 m² pilot system	40 m² PVT	3 - 12	Water-to-water	0.13	19.4
	40 m² small HP	40 m² PVT	1.2 - 6	Water-to-water	0.11	16.4
	20 m² small HP	20 m² PVT	1.2 - 6	Water-to-water	0.11	13.9
	15 m² small HP	15 m² PVT	1.2 - 6	Water-to-water	0.12	14.4
	10 m² small HP	10 m² PVT	1.2 - 6	Water-to-water	0.12	14.5
	40 m² PV air-HP	40 m² PV	1.2 - 6	Air-to-water	0.10	10.7
Greece	Reference system	-	0.9 - 4.5	Air-to-water	0.08	-
	40 m² pilot system	40 m² PVT	3 - 12	Water-to-water	0.09	27.4
	40 m² small HP	40 m² PVT	0.9 - 4.5	Water-to-water	0.07	20.4
	20 m² small HP	20 m² PVT	0.9 - 4.5	Water-to-water	0.07	19.4
	15 m² small HP	15 m² PVT	0.9 - 4.5	Water-to-water	0.08	20.5
	10 m² small HP	10 m² PVT	0.9 - 4.5	Water-to-water	0.08	21.3
	40 m² PV air-HP	40 m² PV	0.9 - 4.5	Air-to-water	0.04	11.3
Austria	Reference system	-	1.2 - 6	Air-to-water	0.10	-
	40 m² pilot system	40 m² PVT	3 - 12	Water-to-water	0.11	29.9
	40 m² small HP	40 m² PVT	1.2 - 6	Water-to-water	0.10	21.7
	20 m² small HP	20 m² PVT	1.2 - 6	Water-to-water	0.09	19.6
	15 m² small HP	15 m² PVT	1.2 - 6	Water-to-water	0.10	20.7
	10 m² small HP	10 m² PVT	1.2 - 6	Water-to-water	0.10	21.0
	40 m² PV air-HP	40 m² PV	1.2 - 6	Air-to-water	0.08	13.5

The LCOE indicator was used to select the best-performing system from a performance and economy perspective among the ones investigated. The reason for choosing LCOE is that it is affected by the system's performance. A lower electricity consumption or a higher electricity self-consumption would result in better performance and lower LCOE. The PP was taken into consideration in cases where two systems had the same LCOE. The best-performing PVT system had 20 m² of PVT area and a smaller HP for all three countries. Further, the study showed that the best-performing PV-HP system had 40 m² of PV area and a smaller HP and lower LCOE and PP than the optimal PVT system. The reason for the difference in panel area between the PVT and the PV systems is the lower price of PV panels and simpler, thus cheaper system installation. Nonetheless, it is clear that the capacity of the HP has to be chosen according to the load it has to operate, regardless of the climate it is installed.

It has to be mentioned that the selected optimal PVT systems did not have the best SPF in any of the investigated countries, contrary to the PV systems, indicating that economy is the main barrier for the PVT-HP systems. However, since the cost of the PVT panels has constantly been decreasing in the last years, it is believed that they will be the best option regarding both performance and economy for cold climates in the near future.

4. Conclusions

In this study, a domestic PVT water-HP system was demonstrated and optimized regarding economy and performance. The system was installed in a single-family house in Ølstykke, Denmark, and measurements from January to July 2019 were presented. A TRNSYS model of the system was created and validated with the measurement data. Afterward, yearly simulations were performed for three different locations, namely Denmark, Greece, and Austria. Three different systems were investigated for each location: a PVT water-source HP, a PV air-source HP, and an air-source HP system. The main findings from this investigation were:

- The best-performing PVT water-source HP system had 22% higher SPF in Denmark, 23% in Austria, and 50% higher in Greece than a PV air-HP system. However, the PV air-source HP system was the most favorable system when considering the economy. The LCOE was 10% lower in Denmark and Austria while 50% lower

in Greece. The main reason is that the investment cost of the PVT water-source HP system is much higher due to the more expensive panels, HP, and installation.

- PVT water-source HP systems have a greater potential in colder climates, where air-source HP systems have a lower SPF, indicating that they could be the optimal option had the system's total price been a little lower.

- In all investigated locations, the best-performing PVT water-source HP system had better performance and economy than the reference system, which was an air-source HP system. The PVT system had 63% higher SPF in Denmark, 64% in Austria, and 125% in Greece. Also, the LCOE was 20% lower in Denmark and 10% lower in Greece and Austria.

- Economy indicators (especially the payback time but also LCOE) improved with higher electricity self-consumption. In general, it is observed that there is no financial benefit from selling electricity to the grid with the listed wholesale electricity prices.

- Proper dimensioning of the HP capacity and collector area is essential for achieving the best economy and performance. However, due to the price difference between the two systems, the selected area for the PV system was 40 m^2 while for the PVT, 20 m^2.

- If the price of the PVT collectors was only 15% higher than PV panels, instead of 30%, which was assumed in this study, then the PVT water-HP systems would have a marginally lower LCOE than the PV air-HP system in Denmark and Austria. This would lead to the PVT water-HP systems having the same, if not better, economy than the PV air-HP systems for cold climates.

In general, it can be stated that the main barrier of the PVT water-source HP systems is the price of the system since they had the highest performance among the studied systems. Since the PVT technology is currently at a relatively early stage in development compared to the more mature PV technology, it is expected that the price of the system will decrease in the future, making the PVT water-HP system the optimal choice regarding performance and economy in cold climates.

5. Acknowledgments

6. References

Daikin, 2017. Daikin UK Price list [WWW Document]. URL https://www.ultimateair.co.uk/downloads/documents-and-guides/Daikin/Sales Catalogues/2017-General-Catalogues/DaikinUK-Heating-Renewables_PriceList_Valid_from_1st_Jan_2017.pdf (accessed 8.5.20).

Daikin, n.d. Technical Data [WWW Document]. URL https://www.termoshop.si/media/SlikeIT/Datoteke/ERLQ-CV3_DATABOOK_ANG2.pdf (accessed 10.1.21).

Danish Utility Regulator, 2019. National Report for Denmark [WWW Document]. URL https://forsyningstilsynet.dk/media/6616/national-report-2019-for-denmark.pdf (accessed 10.1.21).

Dannemand, M., Sifnaios, I., Tian, Z., Furbo, S., 2020. Simulation and optimization of a hybrid unglazed solar photovoltaic-thermal collector and heat pump system with two storage tanks. Energy Convers. Manag. 206. https://doi.org/10.1016/j.enconman.2019.112429

Danny, J., 2018. TRNSYS Type 835 - PV model for the coupling with solar thermal absorber and collector models as PVT model [WWW Document]. URL https://www.researchgate.net/profile/Danny_Jonas/publication/331529583_TRNSYS_Type_835_PV_model_for_the_coupling_with_solar_thermal_absorber_and_collector_models_as_PVT_model/data/5c7e733a4585 15831f855857/Type835-Documentation.pdf (accessed 2.17.22).

EnergiNet, n.d. Tariffs and Fees [WWW Document]. URL https://energinet.dk/El/Elmarkedet/Tariffer (accessed 4.6.20).

Europe-Solarshop, n.d. Fronius Inverters [WWW Document]. URL http://www.europe-solarshop.com/fronius.html?infinite=true& (accessed 5.25.20).

European Commission, 2019. European electricity markets [WWW Document]. URL https://ec.europa.eu/energy/sites/ener/files/documents/quarterly_report_on_european_electricity_markets_q_2_2019_final.pdf (accessed 4.7.20).

Eurostat, 2019. Hourly labour costs [WWW Document]. URL https://ec.europa.eu/eurostat/statistics-explained/index.php/Hourly_labour_costs (accessed 4.7.20).

Fechner, H., 2018. National survey report of PV power applications in Austria [WWW Document]. IEA PVPS Task 1. URL https://iea-pvps.org/wp-content/uploads/2020/01/NSR_Austria_2018.pdf (accessed 5.4.20).

Fina, B., Auer, H., Friedl, W., 2020. Cost-optimal economic potential of shared rooftop PV in energy communities: Evidence from Austria. Renew. Energy 152, 217–228. https://doi.org/10.1016/j.renene.2020.01.031

HAEE, 2019. Greece energy market report [WWW Document]. URL https://www.haee.gr/media/4858/haees-greek-energy-market-report-2019-upload-version.pdf (accessed 4.7.20).

IEA SHC Task 60, n.d. PVT Systems: Application of PVT Collectors and New Solutions in HVAC Systems [WWW Document]. URL http://task60.iea-shc.org/ (accessed 10.1.21).

IEA Task 54, 2018. LCOH for solar thermal applications [WWW Document]. URL http://task54.iea-shc.org/Data/Sites/1/publications/A01-Info-Sheet--LCOH-for-Solar-Thermal-Applications.pdf (accessed 10.1.21).

International Organization for Standardization, 2017. ISO 9806:2017 Solar energy - Solar thermal collectors - Test methods.

Jordan, U., Vajen, K., 2001. Realistic domestic hot-water profiles in different time scales, Report for IEA-SHC Task.

Jordan, U., Vajen, K., 2000. Influence of the DHW profile on the Fractional Energy Savings: A Case Study of a Solar Combi-System. Sol. Energy 69(Suppl.), 197–208.

Lämmle, M., Oliva, A., Hermann, M., Kramer, K., Kramer, W., 2017. PVT collector technologies in solar thermal systems: A systematic assessment of electrical and thermal yields with the novel characteristic temperature approach. Sol. Energy 155, 867–879. https://doi.org/10.1016/j.solener.2017.07.015

PriceRunner [WWW Document], 2020. URL https://www.pricerunner.dk (accessed 10.1.21).

VVS-Eksperten A/S [WWW Document], 2020. URL https://www.vvs-eksperten.dk (accessed 10.1.21).

Wang, K., Herrando, M., Pantaleo, A.M., Markides, C.N., 2019. Technoeconomic assessments of hybrid photovoltaic-thermal vs. conventional solar-energy systems: Case studies in heat and power provision to sports centres. Appl. Energy 254. https://doi.org/10.1016/j.apenergy.2019.113657

Zottl, A., Nordman, R., Miara, M., 2012. Benchmarking method of seasonal performance.